

Determination of the Poloidal Magnetic Field Profiles in a Tokamak by Polarization Spectroscopy of an Impurity Ion Line

D. Wróblewski, L. K. Huang, and H. W. Moos

Department of Physics and Astronomy, The John Hopkins University, Baltimore, Maryland 21218

and

P. E. Phillips

Fusion Research Center, The University of Texas, Austin, Texas 78712

(Received 11 July 1988)

Profiles of the poloidal magnetic field in Ohmically heated, sawtoothed discharges are determined in the Texas Experimental Tokamak (TEXT) from a precise measurement of the partial circular polarization of an impurity-ion line, TiXVII 3834 Å. The sawtooth-period-averaged safety factor (inverse of the rotational transform) on the plasma axis is found to be close to 1.0, independent of its value on the plasma edge. The measurements indicate a decoupling of the current and temperature profiles and a flat current density profile in the center of the discharge.

PACS numbers: 52.55.Fa, 32.60.+i, 52.70.Kz

The knowledge of the poloidal field profile (associated with the toroidal current distribution) is essential for understanding many aspects of the physics of the tokamak device, such as the plasma confinement, stability, and energy balance. Direct measurement of the poloidal field profile has proved to be rather difficult and only few such measurements have been reported. The currently used techniques include the measurement of the polarization of the Zeeman component of a resonance transition from a high-energy lithium beam injected into the plasma,^{1,2} and the measurement of the Faraday rotation of an infrared laser beam.³ A measurement with laser light scattering was also demonstrated⁴ and a number of other methods has been proposed.⁵⁻¹¹

From the point of view of plasma stability, the value of the safety factor in the plasma center, q_0 , is of primary importance ($q \approx B_T r / B_p R$, where B_T is the toroidal magnetic field, B_p is the poloidal magnetic field, R is the major radius, and r is the minor radius coordinate). The theoretical models predict that the $q=1$ surface is unstable to the kink (tearing) instability which leads to a periodic redistribution of the central plasma current and prevents q_0 from falling significantly below 1.^{12,13} This redistribution process is associated with the sawtoothlike oscillations of plasma temperature and density observed in the plasma center.

In the absence of a direct measurement, the current profile may be deduced from the measured electron temperature profile, if we assume the electric field profile (usually constant) and the functional dependence of plasma resistivity on the temperature (e.g., Spitzer or neoclassical). Such a procedure typically yields q_0 significantly smaller than 1 (e.g., 0.6). Although the Kadomtsev model¹² allows a radially nonuniform electric field profile and thus a decoupling of the current and

temperature profiles,¹⁴ measurements of $q_0 < 1$ (e.g., $q_0 = 0.7$ in TEXTOR,³ and $q_0 = 0.7-0.8$ in TEXT²), and of the current profile conforming to the electron temperature profile,¹ have been reported for sawtoothed tokamak discharges.

In this Letter, we present measurements of the poloidal field profiles in the Texas Experimental Tokamak (TEXT), based on a precise analysis of the fractional circular polarization of the TiXVII 3834-Å magnetic dipole line. With use of modest equipment, the technique provides high-quality data. The fractional polarization of the line is measured with accuracy better than 5×10^{-3} which corresponds to an uncertainty of 0.005–0.01 T in the measurement of the line-of-sight-averaged poloidal field.

The theory of the measurement and a detailed description of the apparatus used in this study are presented elsewhere.¹⁵⁻¹⁸ Briefly, the profile of a spectral line emitted from a high-temperature tokamak plasma is dominated by the Doppler (thermal) effect. A small contribution of the Zeeman effect, due to the strong confining magnetic field, results in a small circular polarization of the line. The directly measured quantity is the difference between left-hand [$I_L(\lambda)$] and right-hand [$I_R(\lambda)$] circularly polarized line profiles. For a Gaussian line profile of width $\Delta\lambda_D$ (FWHM), the maximum difference between the circularly polarized profiles (the fractional circular polarization), referred to as the “polarization modulation,” is given by

$$P_{\max} = \max \left[\frac{I_L - I_R}{I_0} \right] \approx 2\sqrt{2} \cos \gamma \frac{\Delta\lambda_B}{\Delta\lambda_D} \sim \lambda_0 \frac{B \cos \gamma}{\sqrt{T_i}}, \quad (1)$$

where γ is the angle between the direction of observation and the total magnetic field, λ_0 is the line wavelength,

$\Delta\lambda_B$ is the Zeeman shift (for the lines considered here, a linear function of the total magnetic field strength), I_0 is the maximum of the unpolarized line profile, and $\Delta\lambda_B/\Delta\lambda_D \ll 1$ was assumed. Thus, the polarization modulation is proportional to the component of the magnetic field in the direction of observation, $B \cos \gamma$.

As the polarization effect increases with the wavelength of the transition, and accurate polarization measurements are not feasible at wavelengths shorter than about 180 nm (transmission cutoff of quartz), long-wavelength lines are the most suitable for the magnetic field measurement. Both the lines due to forbidden (magnetic dipole) transitions within the ground configuration of high ionization stages of heavy impurities,¹⁵ and the lines of hydrogenlike ions of light impurities excited by the charge-exchange recombination with a neutral beam¹⁹ have been suggested for this measurement. The magnetic dipole transition employed in this study, Ti XVII 3834 Å ($2s^2 2p^2 3P_2 \rightarrow 3P_1$), is due to an intrinsic impurity (titanium is contained in the TEXT limiter), which provides the advantage of the line brightness being approximately constant during the steady-state part of the discharge (about 300 ms).

In the polarimeter used in this work,¹⁸ a piezoelectrically driven scanning Fabry-Perot interferometer provides the wavelength resolution of about 1.0 Å, with the line-scan time of about 30 ms. A circular-polarization analyzer, consisting of a photoelastic modulator and a Wollaston prism, allows for a rapid (50 kHz) switching between the left- and right-hand polarized line profiles. The detector (photomultiplier tube) signal is superposition of the slow line profile scan and the 50-kHz modulation with amplitude proportional to the difference between the circularly polarized profiles (\sim poloidal field). Phase-sensitive detection and amplification of the polarization signal allows one to minimize the effect of extraneous noise sources and, together with the large throughput of the Fabry-Perot interferometer and the efficient light-collection and light-transfer optics, provides an adequate signal-to-noise ratio.

The major radius of the TEXT plasma is 1.0 m, and the limiter radius 0.26 m. The plasma is observed vertically through a bottom port. The direction of observation is in the poloidal plane, i.e., perpendicular to the toroidal field. The apparatus provides a measurement for a single line of sight, and the radial profiles are obtained on a shot-to-shot basis by variation of the direction of observation. The window size limits the observation to the low-field (outward) side of the torus. To avoid errors associated with the spurious polarization produced by the optics, the instrument is calibrated during each run by deflection of the line of sight in the toroidal direction and measurement of the signal due to a small component (≈ 0.1 T) of the (known) toroidal field.

Two types of discharges, with different values of the safety factor on the plasma edge, q_a , were studied: (a)

$q_a = 2.0$, $B_T = 1.8$ T and $I_p = 300$ kA (or $B_T = 1.5$ T and $I_p = 250$ kA), and $n_e = (1.0-1.8) \times 10^{13}$ cm⁻³; and (b) $q_a = 3.4$, $B_T = 2$ T, $I_p = 200$ kA, $n_e = (1.0-1.5) \times 10^{13}$ cm⁻³. I_p is the total plasma current, n_e is the line-averaged central electron density, and $q_a \sim B_T a^2 / R I_p$, where R is the major radius and a is the minor radius of the plasma. All of these discharges exhibit the sawtooth oscillations, observed, e.g., in the soft-x-ray emission, with period of the order of 1 ms, much shorter than the line-profile scan (measurement) time. As the poloidal field measurement at a given spatial position is also averaged over, typically, 3-10 shots, the possible variations of the poloidal field associated with the sawtooth instability cannot be resolved.

The excellent reproducibility and consistency of the measurement is demonstrated in Fig. 1, which shows the line-of-sight-averaged poloidal field measured in the central part of discharges with $q_a = 2.0$. The abscissa is the distance, measured on the machine midplane, between the line of sight and the center of the vacuum vessel. In general, we find that the position of the magnetic axis determined with the magnetic field diagnostic ($B_p = 0$ at $x \approx 2.5$ cm in Fig. 1) agrees very well with the position of the center of the sawtooth inversion region obtained with the soft-x-ray diagnostic. For example, the same small difference in the position of the magnetic axis for discharges with slightly different parameters was observed with both diagnostics. An occasional small systematic discrepancy between the two diagnostics may be attributed to a misalignment of the polarimeter line of sight with respect to the poloidal plane, which introduces a bias field due to a small component of the strong toroidal field. The misalignment error is estimated to be

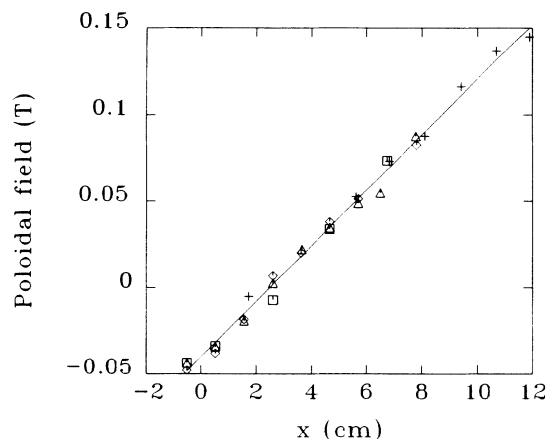


FIG. 1. Measured (line-averaged) poloidal field in the center of the plasma for discharges with $q_a = 2.0$: $B_T = 1.8$ T, $I_p = 300$ kA, and (+) $n_e = 1.4 \times 10^{13}$ cm⁻³, (◇) $n_e = 1.5 \times 10^{13}$ cm⁻³, (□) $n_e = 1.8 \times 10^{13}$ cm⁻³; (Δ) $B_T = 1.5$ T, $I_p = 250$ kA, $n_e = 1.0 \times 10^{13}$ cm⁻³. The data obtained for $B_T = 1.5$ T were multiplied by 1.2. Solid line is the linear least-square fit.

about $\pm 0.2^\circ$, resulting in an uncertainty in the determination of the magnetic axis position of about ± 0.5 cm. Figure 1 shows results of four separate radial scans. The individual scans were recalibrated (by addition or subtraction of a small bias field of up to 100 G) to indicate the same position of the magnetic axis. Note that all the experimental points are very well fitted by a single straight line, implying the same value of q_0 .

The measurements of the poloidal field profiles for discharges with $q_a = 2.0$ and $q_a = 3.4$ are summarized in Figs. 2 and 3, respectively. The poloidal field on the machine midplane is plotted as a function of the Shafranov flux coordinate $\rho = r/a$, where r is the radius of the magnetic surface. The error bars for the experimental points (line-of-sight-averaged result) represent, respectively, the standard deviation of the single-shot measurement from the average of 3–10 shots, and the approximate diameter of the plasma volume from which the radiation is collected. The experimental data points obtained on both sides of the magnetic axis are shown, with the negative-poloidal-field data mirror plotted. The $q_a = 2.0$ data are a superposition of two separate scans: $B_T = 1.8$ T, $I_p = 300$ kA, and $n_e = 1.4 \times 10^{13}$ and $1.5 \times 10^{13} \text{ cm}^{-3}$. The broken line is the fit to the data used in the inversion procedure described below. In the fit, the value assumed for the edge ($\rho = 1$) poloidal field was consistent with the magnitude of the total plasma current.

The emission profile of the titanium line in TEXT is quite broad with measurable brightness extending almost to the plasma edge. Thus, the whole poloidal field profile

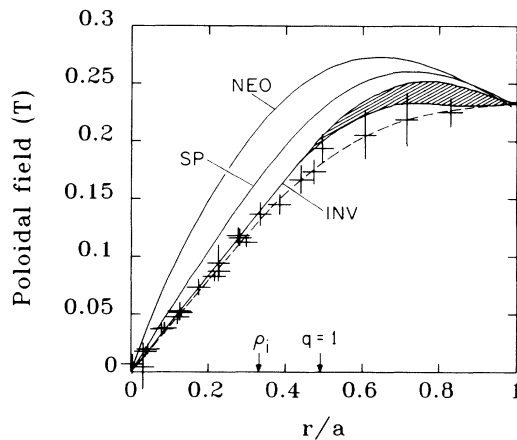


FIG. 2. The poloidal field profile for the discharge with $q_a = 2.0$. The broken line is a fit to the experimental points. The inverted (corrected for the line-of-sight integration) profile (INV) is compared with the profiles calculated from measured electron temperature profiles, assuming Spitzer (SP) or neo-classical (NEO) resistivity. ρ_i is the approximate position of the sawtooth inversion region (soft-x-ray emission diagnostic), and $q = 1$ indicates the boundary of the flat portion of the current profile.

may be determined from this line. On the other hand, the effect of the integration along the line of sight must be taken into account in the interpretation of the measurement. In general, the measured poloidal field (polarization modulation) profile depends on the volume emission profile of the line, the ion temperature profile, and the poloidal field profile. The correction to a measured profile is made with the assumption of a cylindrical geometry of the plasma cross section (with the plasma center at the location of the magnetic axis). The toroidal corrections, due to the fact that the actual magnetic surfaces are not concentric and the poloidal field is not constant on a surface, are estimated to be of the order of only a few percent of the measured field and thus are not taken into account. The measured profiles of line brightness and poloidal field are either directly Abel inverted to yield the profile-of-volume-emission coefficient and the local poloidal field, or an iterative procedure is used in which the (local) poloidal field profile is varied until the line-of-sight-integrated result (including the emissivity and temperature profiles) agrees with the measured profile. For the profiles studied here the measurement is weighted strongly towards the plasma center and the inversion procedure introduces only a small correction to the measured poloidal field (5% to 20%). The inversion results are shown in Figs. 2 and 3. The shaded area indicates uncertainty associated with the determination of the magnetic axis position. Also shown are the poloidal field profiles calculated from the measured profiles of electron temperature, with the assumption of Spitzer or neoclassical resistivity, and Z_{eff} and toroidal electric field independent of the radial position.

The sawtooth-period-averaged safety factor on the plasma axis is determined from the slope of the central portion of the inverted profiles: $q_0 \approx B_T / [R(dB_p/dr)_{r=0}]$. For the presented poloidal field profiles one obtains $q_0 = 0.98 \pm 0.08$ for the discharge with $q_a = 3.4$, and $q_0 = 1.0 \pm 0.10$ for $q_a = 2.0$. The uncertainty is due

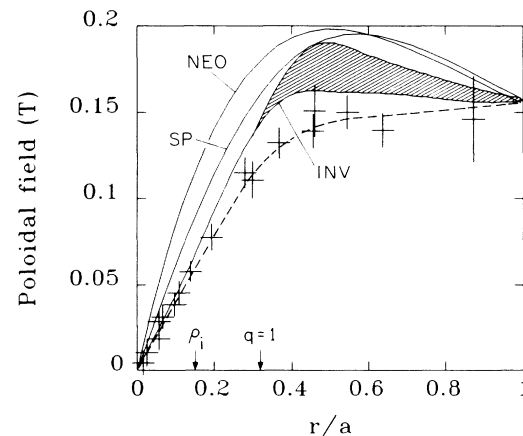


FIG. 3. Same as Fig. 2, but for the discharge with $q_a = 3.4$.

to the calibration error, propagation of the measurement error, and uncertainties associated with the inversion procedure. This result is in agreement with the accepted theory of the sawtooth oscillation but in disagreement, not understood at the present time, with the previously reported measurements.² To our best knowledge, there was no significant difference between the discharges studies in this work and in Ref. 2.

The significant difference between measured and calculated profiles indicates a decoupling of the current profile from the temperature (resistivity) profile. The presented measurements indicate a constant current density in the center of the plasma, with the flat portion wider for the discharge with lower q_a . (A flat portion of the current density profile is identified with the part of the poloidal field profile which is linear in ρ . In our case, this is also the region where $q \approx 1$.) The width of the flat portion appears to be related to the inversion radius of the sawtooth oscillations, r_i , usually identified with the position of the $q = 1$ surface. For $q_a = 3.4$, the inversion radius is determined from the soft-x-ray emission diagnostic to be about 3.5 cm ($\rho_i = r_i/a \approx 0.15$), and the linear portion of the measured poloidal field profile extends to about $2r_i$. For $q_a = 2.0$, $r_i \approx 8$ cm ($\rho_i \approx 0.33$), and the current density appears to be constant within about $1.5r_i$.

We would like to acknowledge the support of the TEXT staff during the course of these experiments. We specially thank A. Wootton and P. Edmonds for making the tokamak available, S. McCool and B. A. Smith for the soft-x-ray diagnostic data, and W. Rowan for useful discussions. This work is supported by U.S. Department

of Energy Grant No. DE-FG02-85ER-53214-A000.

-
- ¹K. McCormick, *et al.*, Phys. Rev. Lett. **58**, 491 (1987).
 - ²W. P. West, D. M. Thomas, J. S. deGrassie, and S. B. Zheng, Phys. Rev. Lett. **58**, 2758 (1987).
 - ³H. Soltwisch, Rev. Sci. Instrum. **57**, 1939 (1986).
 - ⁴M. J. Forrest, P. G. Carolan, and N. J. Peacock, *Nature* (London) **271**, 718 (1978).
 - ⁵R. Cano, I. Fidone, and J. C. Hosea, Phys. Fluids **18**, 1183 (1975).
 - ⁶Equipe TFR, Nucl. Fusion **18**, 647 (1978).
 - ⁷J. D. Strachan, Rev. Sci. Instrum. **56**, 1133 (1985).
 - ⁸TFR Group, Europhys. Lett. **2**, 267 (1986).
 - ⁹F. M. Levinton, Rev. Sci. Instrum. **57**, 1834 (1986).
 - ¹⁰M. Wickham, S. Fornaca, and N. H. Lazar, Rev. Sci. Instrum. **55**, 1748 (1984).
 - ¹¹E. S. Marmor, M. Greenwald, and J. L. Terry, Bull. Am. Phys. Soc. **31**, 1588 (1986).
 - ¹²B. B. Kadomtsev, Fiz. Plazmy **1**, 710 (1975) [*Sov. J. Plasma Phys.* **1**, 389 (1975)].
 - ¹³M. N. Rosenbluth and P. H. Rutherford, in *Fusion*, edited by E. Teller (Academic, New York, 1981), Vol. 1, Part A, p. 31.
 - ¹⁴F. Alladio and G. Vlad, Phys. Fluids **31**, 602 (1988).
 - ¹⁵U. Feldman, J. F. Seely, N. R. Sheeley, Jr., S. Suckewer, and A. M. Title, J. Appl. Phys. **56**, 2512 (1984).
 - ¹⁶D. Wróblewski, H. W. Moos, and W. L. Rowan, Appl. Phys. Lett. **48**, 21 (1986).
 - ¹⁷V. L. Jacobs and J. F. Seely, Phys. Rev. A **36**, 3267 (1987).
 - ¹⁸D. Wróblewski, L. K. Huang, and H. W. Moos, Rev. Sci. Instrum. (to be published).
 - ¹⁹D. Wróblewski and H. W. Moos, Rev. Sci. Instrum. **57**, 2029 (1986).